HHS Public Access

Author manuscript

Biochim Biophys Acta. Author manuscript; available in PMC 2016 September 01.

Published in final edited form as:

Biochim Biophys Acta. 2015 September ; 1852(9): 2000–2012. doi:10.1016/j.bbadis.2015.06.020.

Osteogenic Changes in kidneys of Hyperoxaluric Rats

Sunil Joshi[1], **William L. Clapp**, **Wei Wang**[1], and **Saeed R. Khan**[1,2]

[1]Department of Pathology, Immunology and Laboratory Medicine, University of Florida, Gainesville, Florida

[2]Department of Urology, College of Medicine, University of Florida, Gainesville, Florida

Abstract

Many calcium oxalate (CaOx) kidney stones develop attached to renal papillary subepithelial deposits of calcium phosphate (CaP), called Randall's plaque (RP). Pathogenesis of the plaques is not fully understood. We hypothesize that abnormal urinary environment in stone forming kidneys leads to epithelial cells losing their identity and becoming osteogenic. To test our hypothesis male rats were made hyperoxaluric by administration of hydroxy-l-proline (HLP). After 28 days, rat kidneys were extracted. We performed genome wide analyses of differentially expressed genes and determined changes consistent with dedifferentiation of epithelial cells into osteogenic phenotype. Selected molecules were further analyzed using quantitative-PCR and immunohistochemistry. Genes for runt related transcription factors (RUNX1 and 2), zinc finger protein Osterix, bone morphogenetic proteins (BMP2 and 7), bone morphogenetic protein receptor(BMPR2), collagen, osteocalcin, osteonectin, osteopontin (OPN), matrix-gla-protein (MGP), osteoprotegrin (OPG), cadherins, fibronectin (FN) and vimentin (VIM) were up regulated while those for alkaline phosphatase (ALP) and cytokeratins 10 and 18 were down regulated. In conclusion, epithelial cells of hyperoxaluric kidneys acquire a number of osteoblastic features but without CaP deposition, perhaps a result of down regulation of ALP and up regulation of OPN and MGP. Plaque formation may additionally require localized increases in calcium and phosphate and decrease in mineralization inhibitory potential.

Keywords

Runt related transcription factor; Bone morphogenetic protein; Vimentin; Matrix-glaprotein; Hyperoxaluria; Randall's plaque

Address for Correspondence: Saeed R. Khan, Department of Pathology, Immunology and Laboratory Medicine, College of Medicine, University of Florida, Gainesville, Florida 32610-0275, khan@pathology.ufl.edu.

Part of this research was presented at the 2014, annual meeting of the American Society Nephrology.

Conflict of Interest

The authors have declared that there is no conflict of interest.

INTRODUCTION

Kidney stone formation is a common chronic disease and its life time prevalence is increasing in United States as well as the rest of the world.[1, 2] The increase in stone prevalence is associated with simultaneous escalation in cost of taking care of patients, which has already reached over ten billion dollars/year. But this figure does not include the hidden costs of nephrolithiasis, the impact on renal functions and quality of life.[3] New epidemiological studies also provide the evidence that stone formation is a risk factor for developing hypertension, chronic kidney disease and end stage renal disease.[4–7] Number of stone episodes and surgical interventions is highly correlated with reduction and loss of renal function.[3] Obesity, hypertension, diabetes, chronic kidney disease and metabolic syndrome, all of whom are on the rise, are also risk factors for stone formation in adult population.[5, 8] In the case of pediatric urolithiasis, analysis of PHIS database showed that stone patients had significantly higher odds of hypertension and obesity than the controls.[9]

Calcium oxalate (CaOx) kidney stones develop attached to Randall's plaques (RP), subepithelial deposits of calcium phosphate (CaP) on renal papillary surface, or Randall's plugs, crystal aggregates blocking the terminal collecting ducts.[10–14] The plaques themselves originate deep inside the renal interstitium associated with the basement membranes of loops of Henle, collecting ducts or blood vessels.[15, 16] Mechanisms involved in the initial formation of the RPs are still unclear. Pathogenesis is generally considered a passive, unregulated physicochemical process.[17] In our opinion,[18] as well as some others[19] plaque and stone formation are actively regulated processes similar to vascular calcification in the kidneys in which vascular smooth cells (VSMC) acquire osteogenic phenotype.[20–22] Exposure of VSMC to elevated levels of calcium and phosphate triggers osteogenic transformation of VSMC.[23–26] Transformation involves increased expression of osteoblast specific genes and decrease in smooth muscle cell markers.[27, 28] Bone morphogenetic proteins, BMP 2 and BMP 4, and Wnt signaling pathways are activated through up-regulation of transcription factor, Runt-related transcription factor 2 (RUNX2). Cells produce matrix proteins. Reactive oxygen species are likely involved in the VSMC transformation to osteogenic phenotype by regulating RUNX-2 transcription factor.[29, 30] It is our hypothesis that abnormal urinary environment such as hyperoxaluria, hypercalciuria and hypocitraturia and associated oxidative stress, produce specific changes in the renal epithelial cells. The cells lose their epithelial character and become osteogenic. We decided to test our hypothesis in a rat model of hyperoxaluria. Since many genes and pathways are involved we performed genome wide analysis of differentially expressed genes in the kidneys and determined changes consistent with the dedifferentiation of epithelial cells into bone producing cells.

We investigated the expression of genes considered to be involved in epithelial transformation and bone morphogenesis including runt related transcription factors (RUNX),[31, 32] zinc finger protein Osterix,[33] bone morphogenetic proteins (BMP1-7), [34] bone morphogenetic protein receptor(BMPR),[35] collagens,[36] alkaline phosphatase (ALP),[37] osteocalcin,[31] osteonectin,[38] osteopontin (OPN), [39] matrix-gla-protein (MGP),[21] osteoprotegrin (OPG),[40] cytokeratins,[41] cadherins,[42] fibronectin (FN) [43]and vimentin (VIM).[44] Epithelial cells express high levels of cytokeratin 8, 10, 18, as

well as E-cadherin, while mesenchymal cells express N-cadherin, fibronectin and vimentin.[45] BMPs play significant role in osteoblast differentiation and interact with BMPRs.[46, 47] Collagens are major constituent of extracellular matrix,[48] control matrix remodeling and are involved in calcification [49] including growth of Randall's plaques.[50] ALP is a membrane associated enzyme and plays critical role in both physiological and pathological calcification.[51, 52] RUNX2 also known as core-binding factor alpha-1 is a key transcription factor associated with osteoblast differentiation.[53, 54] Osterix is a zinc-finger containing transcription factor essential for osteoblast differentiation.[46] This report shows the changes that occur in the expressions of these molecules of interest in renal tissues in response to sustained hyperoxaluria and crystal formation. We discuss how these changes point to a number of molecular processes that may be involved in the deposition of CaP crystals in the renal interstitium and formation of plaques.

MATERIALS AND METHODS

Animal Procedures

The experiments described herein were performed in Sprague-Dawley rats purchased from Harlan Labs, Inc. The studies were approved by the University of Florida's IACUC and were conducted in accordance with the recommendations of the NIH Guide for the Care and Use of Laboratory Animals. All procedures are detailed in our earlier publications.[55–57] In brief, two groups of 6 rats each, average weight of 150 grams, were placed in metabolic cages with free access to food and water. Rats in group 1 were fed a normal rat chow diet and given sterile water. Rats in group 2 were fed the same chow as group 1 rats, but supplemented with 5% (w/w) hydroxy-l-proline (HLP). At the end of day 28, all rats were euthanized and their kidneys removed. From each rat, one kidney was used for RNA isolation, while the second was placed in 10% phosphate buffered formalin for histological analyses.

RNA extraction and differential expression of genes by microarray analysis

Each rat kidney excised for RNA isolation was surgically separated into medulla and cortex, then snap frozen in liquid nitrogen and stored at −80°C. Total RNA was isolated concurrently from each of the specimens using the RNeasy Mini-Kit (QIAGEN, Valencia, CA) as per the manufacturer's instructions. Microarray hybridizations were carried out with each of the RNA specimens using the Illumina™RatRef-12 Expression Bead Chip containing >22,000 genes expressed in the rat genome. Expressed values were determined using the Illumina™ bead array reader. All microarray data have been deposited with the Gene Expression Omnibus (GSE36446).

Gene expression data analysis was performed using the Genome Studio Gene Expression Module V1.0. Before the analysis, the individual signal intensity values retrieved from the microarray probes were log transformed (using 2 as a base) and normalization was done for all the individual samples within each study group. After normalizing the signal intensity values for each of the 36 arrays, the Student's t-test was used to do a probe-by probe comparison between two groups concurrently. For each comparison, the fold change (FC) and p-value was calculated for each gene within each experimental group and volcano plots

were drawn for each comparison. Differential gene expressions were compared between the cortex and medulla tissues from control versus HLP-treated rats using Database for Annotation, Visualization of Integrated Discovery (DAVID) enrichment analysis tool (Bioinformatics Resources, National Institute of Allergy and Infectious Diseases) for GO: TERM and KEGG pathway analysis. [58, 59] Cluster analysis of genes was also done for the identification of biological processes, cellular component, and molecular function ontology.

Histological examinations

Formalin fixed tissues were embedded in paraffin and sectioned to a thickness of 5-μm. Deparaffinization of paraffin-embedded slides was performed by xylene immersion followed by dehydration in ethanol. Kidney sections were stained with Hematoxylin/ Eosin (H&E) and periodic acid-Schiff (PAS). Immunohistochemical staining was performed using specific antibodies against VIM, collagen, OPN, MGP, FN and pancytokeratin antibody AE1/3, a cocktail for a number of cytokeratins found in epithelial cells. Staining was developed by the addition of diaminobenzidine (DAB) substrate (Vector Labs, Burlingame, CA, USA) and counterstained with hematoxylin. Images were taken using the Zeiss Axiovert 200M microscope (Carl Zeiss Microimaging, Inc., Thornwood, NY, USA).

Real Time-PCR

Results of microarray analyses were confirmed using RT-PCR of selected genes. cDNA was generated using Invitrogen's SuperScript III First-Strand Synthesis System (Carlsbad, CA, USA; Cat. # 18080-051), as described previously.[55] Quantitative real time PCR was carried out to determine the mRNA expression of fibronectin1 (Fn1), runt related transcription factor-2 (RUNX2), Osterix, bone morphogenetic proteins (BMP2, BMP7), bone morphogenetic protein receptor, Type 2 (BMPr2), cytokeratins (KRT8, KRT18), VIM, OPN, CoL1a1, and ALP in both renal cortex and medulla. The mRNA of these genes was PCR amplified and detected using the Roche's FastStart High Fidelity PCR System (Indianapolis, IN, USA; Cat. # 03553426001). Housekeeping genes GAPDH and Actin were used to normalize the expression of the tested genes. These stable housekeeping or the internal control genes were used to remove any sampling differences (such as RNA quantity and quality) in order to identify real gene expression. The forward and reverse primers used are listed in Table 1.

“cDNA was generated using Invitrogen's SuperScript III First-Strand Synthesis System (Carlsbad, CA, USA; Cat. # 18080-051). Briefly, 5 μg of total RNA was added to a 0.5-mL tube with 50 μM Oligo (DT) 20, 10 mM dNTP mix, and DEPC-treated water for a final volume of 10 μL. The sample was incubated at 60°C for 5 min and then placed on ice for 1 min. The sample was then added to cDNA Synthesis Mix [10 × RT buffer (supplied with kit), 25 mM MgCl2, 0.1 M DTT, 40 U/μL RNase OUT, 200 U/μL SuperScript III RT] and incubated at 50°C for 50 min. The reaction was terminated by heating at 85°C for 5 min followed by chilling on ice. One microliter of Rnase H was added to samples and incubated for 20 min at 37°C. After incubation, the samples were ready for use in RT-PCR reaction.”

Real time RT-PCR was performed using the SYBR® Green PCR master Mix (Cat. # 4309155) and the Applied Biosystems StepOnePlusTM Real Time PCR systems to determine the gene expression. PCR reactions were performed in total volume of 20 μL containing 10 μL of SYBR® Green PCR master Mix, 1 μL of forward and reverse primer each, 4 μL of cDNA, and 4 1 μL of sterile DD H2O. The reactions were cycled for 950C for 10 min, followed by 40 × cycles of 950C for 15 min, 600C (for RUNX2, SP7, ALP, BMP2, KRT8, VIM,Fn1 and Col1A1) or 550C (for BMP7, BMPr2) or 650C (for KRT18) or 630C (for OPN) for 1 min.

RESULTS

Histology

HLP administration to male rats produced hyperoxaluria and CaOx crystal deposition in their kidneys as shown previously. [55, 56, 60] After 28 days of HLP consumption, urinary excretion of oxalate by the rats was many folds higher than the controls and extent of crystal deposition ranged from few small crystal aggregates to extensive deposition of large deposits throughout the kidneys. Even though renal tubules of all segments of the kidneys, cortex, medulla and papilla, contained CaOx crystals, the majority of the crystals were seen in the tubular lumens of the distal tubules and collecting ducts of the cortex and outer medulla (Figure 1). The tubular segments that contained crystals were dilated with many fold increase in lumen diameter. Their lining epithelium appeared damaged. Tubular epithelia were attenuated and focally sloughed from the tubular basement membranes. Interstitial inflammation was conspicuous around the tubules containing crystals. Glomeruli and tubules without crystals appeared normal.

Microarray Analysis

Relative gene expression of runt related transcription factor-1 and 2 (RUNX1 and RUNX2), and zinc finger protein Osterix/SP7 was greatly up regulated in both the renal cortex and medullary tissues of the HLP-fed rats compared to the tissues from the control rats (Figure 2). Expression of gene for ALP was down regulated (Figure 2). Relative gene expression of bone morphogenetic proteins 2 and 7 (BMP2 and BMP7), and bone morphogenetic protein receptor Type 2 (BMPR2) were also up regulated in the kidneys of the HLP- fed rats (Figure 3). Relative expression of genes for cytokeratin 10 (KRT 10) and cytokeratin 18 (KRT 18) were down regulated while that of cytokeratin 8 (KRT 8) up regulated in both the cortex and medulla of HLP-treated rat kidneys (Figure 4). Relative expression of gene encoding for VIM was also highly up regulated in kidneys of the HLP treated rats as shown in Figure 4.

Osteoblast marker genes, encoding for OPN, FN, COL1a1, COL1a2 (Figure 5), osteocalcin, bone differentiation marker osteonectin (results not shown) were also upregulated. Similarly there were significant increases in gene encoding for MGP (results not shown). Genes for osteoblast secreted receptor osteoprotegrin (OPG) and cadherins 1, 10, 16, which are involved in regulating cell adhesion and mobility, were all down regulated (results not shown).

Real Time PCR

Results of microarray analyses were confirmed by performing RT-PCR for selected molecules. Both RUNX2 and Osterix mRNA showed many fold increases in both the cortex and medulla of the HLP-treated rat kidneys (Figure 6). There was many fold reduction in alkaline phosphatase mRNA, a very important player in calcification, in both the cortex and medulla of hyperoxaluric rat kidneys compared to the control (Figure 6).

mRNA's of bone morphogenetic proteins BMP2, BMP7, and their receptor BMPR2 were also increased in both the cortex and medulla of the treated rats (Figure 7). Figure 8 shows results of real time PCR of cytokeratin 8 (KRT8), cytokeratin 18 (KRT18), and Vimentin (VIM) in the cortex and medulla of the control and HLP fed rats. Expression of cytokeratin 8 mRNA increased while that of 18 decreased in both cortical and medullary tissues. There was many fold increase in VIM mRNA in HLP treated rat kidneys.

There were many fold increases in mRNA expression for OPN, Fn1, Col1a1 in both the cortex and medulla of the hyperoxaluric rats compared to the control tissues (Figure 9). MGP mRNA expression was similarly increased (results not shown).

Immunohistochemistry

Vimentin is an intermediate filament expressed mostly in mesenchymal cells. Vimentin staining in normal kidneys was limited to the podocytes and mesangial cells of the glomeruli and endothelium of the peritubular capillaries in the cortex and vasa recta of the renal medulla (Figure 10 A,B). Tubular epithelia in both cortex and medulla were generally devoid of vimentin staining. The papillary surface urothelium of the normal kidneys was also not stained. There was increased vimentin immunoreactivity in the kidneys of hyperoxaluric rats with CaOx nephrolithiasis. Almost all elements of the kidney including the renal interstitium and most renal tubules showed vimentin staining. Strong vimentin expression was seen in tubules that contained CaOx crystals (Figure 10 C,D). Papillary surface urothelium and both the cortical and medullary collecting ducts that did not contain CaOx crystals lacked vimentin expression.

Pancytokeratin antibody AE1/3 is a cocktail for a number of cytokeratins found in epithelial cells. No obvious difference was visible in staining patterns between the kidneys of the control and rats with CaOx nephrolithiasis (Figure 10 E,F). Glomeruli, endothelium of the peritubular capillaries and vasa recta and proximal tubules were negative for pancytokertain. The papillary surface urothelium and epithelia of the collecting ducts, distal tubules, and thin limbs of the loops of Henle were generally positively stained.

Figure 11 shows images of normal and hyperoxaluric kidneys stained for collagen. In the normal kidneys, Collagen 1 staining was mostly seen around the large and small blood vessels (Figure 11A). Staining increased in kidneys of hyperoxaluric rats (Figure 11 B, C) particularly around the tubules that contained CaOx crystals. Collagen stained blue with Masson's trichrome, around the dilated renal tubules that contained CaOx crystals (Figure 11D). Epithelial cells of renal tubules without crystals stained red and their nuclei, dark brown.

Figure 12 shows staining for OPN, fibronectin and MGP. Normal kidneys showed nonspecific, infrequent and light staining for these macromolecules (Figures 12 A, C, E). Heavy OPN expression was mostly associated with the crystal deposits (Figure 12D). Luminal surfaces of the tubular epithelial cells in contact with the crystals were heavily stained compared to their lightly stained cytoplasm. Fibronectin staining was seen in the renal tubular epithelial cells, their lumens as well as peritubular spaces (Figure 12 F). Matrix gla protein expression was most pronounced in the medullary peritibular vessels (Figure 12 B) in the kidneys of the hyperoxaluric rats. It was also seen associated with CaOx crystals deposits and the epithelial cells in contact with the crystals. Normal kidneys showed no staining or non specific staining of the tubular contents (Figure 12A).

DISCUSSION

It is generally agreed that Randall's plaques, the sub-epithelial deposits of CaP on renal papillary surfaces, act as nidi for the development of at least some idiopathic CaOx kidney stones.[10, 14, 61] Pathogenesis of the plaques, where and how do they begin and grow, is however not well understood. The observations that stone formation and cardiovascular diseases such as hypertension, myocardial infarction, carotid artery atherosclerosis, coronary heart disease,[4, 5, 62, 63] often co-exist and share risk factors, markers and outcomes have led us to hypothesize that similar molecules and pathways may be involved in vascular calcification and RP formation.[5, 64] The mechanism of calcification is complicated, but results of multiple investigations suggest it to include a competition between pro- and anti-mineralizing factors. In the case of vascular calcification, one of the best studied processes, first step appears to be transformation of vascular smooth cells into an osteoblast/chondrocyte phenotype.[21] *In vitro* studies have shown that exposure of VSMC to elevated levels of calcium and phosphate [23–26] or uremic toxins such as oxidized proteins, and lipids[65] can trigger transformation and accelerate calcification. We hypothesize that high oxalate and CaOx crystals can similarly trigger epithelial to osteoblast transformation. But it alone cannot explain the formation of Randall's plaques, which are common even in non-stone formers.[10, 12] There is the possibility of other instigators and situations, such as reduction in crystallization inhibitory capacity as shown in THP null mice.[66] Lack of overt inflammation around the plaques would also indicate malfunctioning crystal clearance system. Experimental studies have shown that crystals, CaOx as well as CaP, provoke inflammatory responses, attract monocytes and macrophages which surround the crystals and eventually dispose of them.[67–70]

Previous *in vitro* cell culture and *in vivo* animal model studies have already shown that renal epithelial cells react to the presence of high oxalate and CaOx/CaP crystals.[71–76] The response is probably mediated by the production of reactive oxygen species[77, 78] through mitochondria [79–82] or NADPH oxidase [57, 83, 84] involvement and characterized by altered expression of specific genes encoding for transcriptional activators, regulators of the extracellular matrix, and growth factors. [85, 86] The production of pro and anti-inflammatory molecule, including OPN, Tamm-Horsfall protein, monocyte chemoattractant-1 (MCP-1), prostaglandin E2 (PGE2), bikunin and other components of inter-α-inhibitor (IαI), α-1 microglobulin, CD-44, calgranulin, heparin sulfate, fetuin, osteonectin, fibronectin and matrix-gla-protein (MGP) is modified.[60, 71, 87] Genes

encoding for fibronectin, CD-44, fetuin B, osteopontin, and matrix-gla protein, are up-regulated while those encoding for heavy chains of inter-alpha-inhibitor 1, 3 and 4, calgranulin B, prothrombin, and Tamm-Horsfall protein were down-regulated.[88] Gene expression of vimentin, a mesenchymal marker, is also increased.[89]

Interestingly, the inflammatory molecules altered during CaOx nephrolithiasis and epithelial exposure to oxalate and CaOx crystals, [71, 87, 88] are also integral to the calcification cascade during both the physiological and pathological processes.[49] Production of OPN, FN, MGP, and collagens are indicators of osteoblastic character of the cells. Results presented here show up-regulation of genes for OPN, FN, MGP and collagens and their increased expression in the kidneys of hyperoxaluric rats indicate transformation of cells from their normal epithelial phenotype to osteoblast.

Transformation of vascular smooth cells into an osteoblast/chondrocyte phenotype is brought about through the up regulation of RUNX2 induced by multiple risk factors including oxidative stress and inflammation.[90] RUNX2 is considered master transcription factor for osteoblast differentiation and matrix production while Osterix works downstream of RUNX2.[53] RUNX1 also appears to be involved in osteogenesis and works in co-operation with RUNX2.[91] In our study, both genome wide analyses and RT-PCR showed that genes responsible for these three transcription factors were up regulated in kidneys of the hyperoxaluric rats.

Bone morphogenetic proteins 2–7 (BMP2-7) belong to transforming growth factor beta superfamily of growth factors and interact with specific receptors, BMPRs on the cell surfaces. BMP2 and BMP7 interact with BMPR2 and are involved in a variety of cellular functions including osteoblast differentiation.[46, 47] RUNX2 is a common target of BMP2. [92, 93] Results of our study show up regulation of BMP2, BMP7 as well as BMPR2 genes in the kidneys of hyperoxaluric rats. BMP2 induces OPN expression through RUNX2.[93] RUNX2 is also involved in transcriptional regulation of many other proteins involved in mineralization such as matrix-GLA protein (MGP),[94] collagen1a1,[95, 96] osteocalcin, [97] and fibronectin.[92] BMP2 and RUNX2 induced calcification is modulated through NADPH oxidase mediated production of reactive oxygen species.[29, 98]

Whether oxalate or CaOx crystals were responsible for altered expressions is difficult to say in this model. However, expression of various genes studied, was higher in the medulla than in the cortex while more crystals were seen in the cortex than in the medulla.

Demonstration of increased gene and protein expression of OPN, FN and MGP in animal model of CaOx nephrolithiasis and cell culture studies is not new. However, upregulation of genes encoding for RUNX1 and 2, Osterix, BMP2 and 7, BMPr2 and Col1a1 and 2 in response to oxalate and/or CaOx crystal exposures and transformation of renal epithelial cells into osteoblast has not been previously reported. A recent study has however, shown high basal levels of BMP2, RUNX2, and Osterix in kidneys of genetic hypercalciuric rat kidneys with intratubular calcium phosphate deposits.[99] Vitamin D receptor (VDR) knockdown in the rats reduced the expression levels of BMP2, RUNX2, and Osterix as well

as CaP crystal deposition in the kidneys. Authors concluded that VDR might be a significant regulator of nephrocalcinosis in genetic hypercalciuric rats.

Our investigations demonstrate upregulation of many key osteogenic genes and proteins involved in calcification, and down regulation of epithelial markers, indicating that renal epithelial cells in hyperoxaluric conditions lose their epithelial phenotype and acquire characteristic features of osteoblasts. That epithelial cells transform into other cell types is well known. Epithelial to mesenchymal transformation is known to play a role in renal fibrosis [100] and mesenchymal stem cells are known to promote calcification.[101] But we did not find any calcium phosphate deposition, intratubular or interstitial, in the kidneys of the hyperoxaluric rats. Actually, none of the experimental rat or mice models of hyperoxaluria have ever reported calcium phosphate crystal deposition in the kidneys.[102, 103] Our study also showed down regulation of alkaline phosphatase and upreguation of calcification inhibitors, OPN and MGP. We deduce that lack of calcium phosphate deposition in the kidneys is related to decrease in the production of alkaline phosphatase which hydrolyses pyrophosphate to provide inorganic phosphate for the formation of CaP crystals. Increased production of OPN and MGP, key inhibitors of crystal formation may also play a role. We postulate that pathogenesis of kidney stones involves renal tubular epithelial cells becoming osteogenic and production and activation of alkaline phosphatase. Deposition of CaP in the renal tubules will lead to the formation of Randall's plugs. Transcytosis of intratubular CaP crystals from the apical to the basal aspect of the epithelium will lead to the formation of Randall's plaques.[72, 104] Both plugs and plaques can act as nidi for the formation of CaOx kidney stones.[10, 14]

Results of our studies indicate the possibility of tubular cells acquiring an osteoblast phenotype after a metabolic stimulus. Despite the osteogenic transformation of the epithelial cells, apatite deposition was not observed indicating the necessity of additional stimuli, alterations, or perhaps involvement of the elements of vascular system.[62] It should also be pointed out that animal models have limitations.[102, 103] For example rats and mice have unipapillate kidneys; may metabolize oxalate differently; and compared to humans, normally excrete very high amounts of oxalate in the urine, without CaOx crystalluria or crystal deposition in the kidneys. Rats and mice appear to possess protective capabilities. Down regulation of alkaline phosphatase seen in this model may be one such response.

Conclusion

Present study represents the first robust demonstration of the possible evolution of tubular cells to osteoblast-like cells. We conclude that hyperoxaluria can induce epithelial cells to acquire a number of osteoblastic characteristics. But those changes are not sufficient to produce deposition of calcium phosphate, which may require additional changes including localized increase in calcium and phosphate and decrease in mineralization inhibitory potential.

Supplementary Material

Refer to Web version on PubMed Central for supplementary material.

ACKNOWLEDGEMENTS

The authors appreciate Dr. Jin Yao, Ms. Ginger Clark, and Dr. Yijun Sun efforts from the University of Florida's Interdisciplinary Center for Biotechnology Research (ICBR) for running the microarrays and providing expert assistance in data analyses. The funding for the research was provided by National Institute of Health (NIH) grant numbers RO1-DK078602 and RO1 DK092311.

Abbreviations

CaOx	calcium oxalate
CaP	calcium phosphate
RP	Randall's plaque
RUNX	Runt-related transcription factor
BMP	bone morphogenetic protein
BMPR	bone morphogenetic protein receptor
ALP	alkaline phosphatase
OPN	osteopontin
MGP	matrix-gla-protein

REFERENCES

1. Stamatelou KK, Francis ME, Jones CA, Nyberg LM, Curhan GC. Time trends in reported prevalence of kidney stones in the United States: 1976–1994. Kidney Int. 2003; 63:1817–1823. [PubMed: 12675858]
2. Scales CD Jr, Smith AC, Hanley JM, Saigal CS. Prevalence of kidney stones in the United States. Eur Urol. 2012; 62:160–165. [PubMed: 22498635]
3. Kartha G, Calle JC, Marchini GS, Monga M. Impact of stone disease: chronic kidney disease and quality of life. Urol Clin North Am. 2013; 40:135–147. [PubMed: 23177641]
4. Rule AD, Roger VL, Melton LJ 3rd, Bergstralh EJ, Li X, Peyser PA, Krambeck AE, Lieske JC. Kidney stones associate with increased risk for myocardial infarction. J Am Soc Nephrol. 2010; 21:1641–1644. [PubMed: 20616170]
5. Khan SR. Is oxidative stress, a link between nephrolithiasis and obesity, hypertension, diabetes, chronic kidney disease, metabolic syndrome? Urol Res. 2012; 40:95–112. [PubMed: 22213019]
6. Jungers P, Joly D, Barbey F, Choukroun G, Daudon M. ESRD caused by nephrolithiasis: prevalence, mechanisms, and prevention. Am J Kidney Dis. 2004; 44:799–805. [PubMed: 15492945]
7. Rule AD, Bergstralh EJ, Melton LJ 3rd, Li X, Weaver AL, Lieske JC. Kidney stones and the risk for chronic kidney disease. Clin J Am Soc Nephrol. 2009; 4:804–811. [PubMed: 19339425]
8. Obligado SH, Goldfarb DS. The association of nephrolithiasis with hypertension and obesity: a review. Am J Hypertens. 2008; 21:257–264. [PubMed: 18219300]
9. Kokorowski PJ, Routh JC, Hubert KC, Graham DA, Nelson CP. Association of urolithiasis with systemic conditions among pediatric patients at children's hospitals. J Urol. 2012; 188:1618–1622. [PubMed: 22906655]
10. Khan SR, Canales BK. Unified theory on the pathogenesis of Randall's plaques and plugs. Urolithiasis. 2015; 43(Suppl 1):109–123. [PubMed: 25119506]
11. Randall A. The Origin and Growth of Renal Calculi. Ann Surg. 1937; 105:1009–1027. [PubMed: 17856988]

12. Randall A. The etiology of primary renal calculus. International Abstract of Surgery. 1940; 71:209–240.
13. Khan SR, Finlayson B, Hackett R. Renal papillary changes in patient with calcium oxalate lithiasis. Urology. 1984; 23:194–199. [PubMed: 6695491]
14. Linnes MP, Krambeck AE, Cornell L, Williams JC Jr, Korinek M, Bergstralh EJ, Li X, Rule AD, McCollough CM, Vrtiska TJ, Lieske JC. Phenotypic characterization of kidney stone formers by endoscopic and histological quantification of intrarenal calcification. Kidney Int. 2013; 84:818–825. [PubMed: 23698231]
15. Evan AP, Lingeman JE, Coe FL, Parks JH, Bledsoe SB, Shao Y, Sommer AJ, Paterson RF, Kuo RL, Grynpas M. Randall's plaque of patients with nephrolithiasis begins in basement membranes of thin loops of Henle. J Clin Invest. 2003; 111:607–616. [PubMed: 12618515]
16. Low RK, Stoller ML. Endoscopic mapping of renal papillae for Randall's plaques in patients with urinary stone disease. J Urol. 1997; 158:2062–2064. [PubMed: 9366312]
17. Halperin ML, Cheema Dhadli S, Kamel KS. Physiology of acid-base balance: links with kidney stone prevention. Semin Nephrol. 2006; 26:441–446. [PubMed: 17275581]
18. Khan SR, Glenton PA, Backov R, Talham DR. Presence of lipids in urine, crystals and stones: implications for the formation of kidney stones. Kidney Int. 2002; 62:2062–2072. [PubMed: 12427130]
19. Gambaro G, D'Angelo A, Fabris A, Tosetto E, Anglani F, Lupo A. Crystals, Randall's plaques and renal stones: do bone and atherosclerosis teach us something? J Nephrol. 2004; 17:774–777. [PubMed: 15593050]
20. Moe SM, Chen NX. Mechanisms of vascular calcification in chronic kidney disease. J Am Soc Nephrol. 2008; 19:213–216. [PubMed: 18094365]
21. Shanahan CM. Vascular calcification. Curr Opin Nephrol Hypertens. 2005; 14:361–367. [PubMed: 15931005]
22. Briet M, Burns KD. Chronic kidney disease and vascular remodelling: molecular mechanisms and clinical implications. Clin Sci (Lond). 2012; 123:399–416. [PubMed: 22671427]
23. Jono S, McKee MD, Murry CE, Shioi A, Nishizawa Y, Mori K, Morii H, Giachelli CM. Phosphate regulation of vascular smooth muscle cell calcification. Circ Res. 2000; 87:E10–E17. [PubMed: 11009570]
24. Kapustin AN, Davies JD, Reynolds JL, McNair R, Jones GT, Sidibe A, Schurgers LJ, Skepper JN, Proudfoot D, Mayr M, Shanahan CM. Calcium regulates key components of vascular smooth muscle cell-derived matrix vesicles to enhance mineralization. Circ Res. 2011; 109:e1–e12. [PubMed: 21566214]
25. Kapustin AN, Shanahan CM. Calcium regulation of vascular smooth muscle cell-derived matrix vesicles. Trends in cardiovascular medicine. 2012; 22:133–137. [PubMed: 22902179]
26. Shanahan CM, Crouthamel MH, Kapustin A, Giachelli CM. Arterial calcification in chronic kidney disease: key roles for calcium and phosphate. Circ Res. 2011; 109:697–711. [PubMed: 21885837]
27. Shroff RC, Shanahan CM. The vascular biology of calcification. Seminars in dialysis. 2007; 20:103–109. [PubMed: 17374082]
28. Jono S, Shioi A, Ikari Y, Nishizawa Y. Vascular calcification in chronic kidney disease. Journal of bone and mineral metabolism. 2006; 24:176–181. [PubMed: 16502129]
29. Byon CH, Javed A, Dai Q, Kappes JC, Clemens TL, Darley-Usmar VM, McDonald JM, Chen Y. Oxidative stress induces vascular calcification through modulation of the osteogenic transcription factor Runx2 by AKT signaling. J Biol Chem. 2008; 283:15319–15327. [PubMed: 18378684]
30. Sun Y, Byon CH, Yuan K, Chen J, Mao X, Heath JM, Javed A, Zhang K, Anderson PG, Chen Y. Smooth muscle cell-specific runx2 deficiency inhibits vascular calcification. Circ Res. 2012; 111:543–552. [PubMed: 22773442]
31. Ducy P, Zhang R, Geoffroy V, Ridall AL, Karsenty G. Osf2/Cbfa1: a transcriptional activator of osteoblast differentiation. Cell. 1997; 89:747–754. [PubMed: 9182762]
32. Kern B, Shen J, Starbuck M, Karsenty G. Cbfa1 contributes to the osteoblast-specific expression of type I collagen genes. J Biol Chem. 2001; 276:7101–7107. [PubMed: 11106645]

33. Zhu F, Friedman MS, Luo W, Woolf P, Hankenson KD. The transcription factor osterix (SP7) regulates BMP6-induced human osteoblast differentiation. Journal of cellular physiology. 2012; 227:2677–2685. [PubMed: 21898406]
34. Hartigan N, Garrigue-Antar L, Kadler KE. Bone morphogenetic protein-1 (BMP-1). Identification of the minimal domain structure for procollagen C-proteinase activity. J Biol Chem. 2003; 278:18045–18049. [PubMed: 12637537]
35. Roberts KE, McElroy JJ, Wong WP, Yen E, Widlitz A, Barst RJ, Knowles JA, Morse JH. BMPR2 mutations in pulmonary arterial hypertension with congenital heart disease. The European respiratory journal : official journal of the European Society for Clinical Respiratory Physiology. 2004; 24:371–374.
36. Ducy P, Desbois C, Boyce B, Pinero G, Story B, Dunstan C, Smith E, Bonadio J, Goldstein S, Gundberg C, Bradley A, Karsenty G. Increased bone formation in osteocalcin-deficient mice. Nature. 1996; 382:448–452. [PubMed: 8684484]
37. Sun H, Ye F, Wang J, Shi Y, Tu Z, Bao J, Qin M, Bu H, Li Y. The upregulation of osteoblast marker genes in mesenchymal stem cells prove the osteoinductivity of hydroxyapatite/tricalcium phosphate biomaterial. Transplantation proceedings. 2008; 40:2645–2648. [PubMed: 18929827]
38. Jundt G, Berghauser KH, Termine JD, Schulz A. Osteonectin--a differentiation marker of bone cells. Cell Tissue Res. 1987; 248:409–415. [PubMed: 3581152]
39. Wesson JA, Johnson RJ, Mazzali M, Beshensky AM, Stietz S, Giachelli C, Liaw L, Alpers CE, Couser WG, Kleinman JG, Hughes J. Osteopontin is a critical inhibitor of calcium oxalate crystal formation and retention in renal tubules. J Am Soc Nephrol. 2003; 14:139–147. [PubMed: 12506146]
40. Wan M, Shi X, Feng X, Cao X. Transcriptional mechanisms of bone morphogenetic protein-induced osteoprotegrin gene expression. J Biol Chem. 2001; 276:10119–10125. [PubMed: 11139569]
41. Chen X, Whitney EM, Gao SY, Yang VW. Transcriptional profiling of Kruppel-like factor 4 reveals a function in cell cycle regulation and epithelial differentiation. Journal of molecular biology. 2003; 326:665–677. [PubMed: 12581631]
42. Juliano RL. Signal transduction by cell adhesion receptors and the cytoskeleton: functions of integrins, cadherins, selectins, and immunoglobulin-superfamily members. Annual review of pharmacology and toxicology. 2002; 42:283–323.
43. Alves RD, Eijken M, Swagemakers S, Chiba H, Titulaer MK, Burgers PC, Luider TM, van Leeuwen JP. Proteomic analysis of human osteoblastic cells: relevant proteins and functional categories for differentiation. Journal of proteome research. 2010; 9:4688–4700. [PubMed: 20690663]
44. Challa AA, Stefanovic B. A novel role of vimentin filaments: binding and stabilization of collagen mRNAs. Molecular and cellular biology. 2011; 31:3773–3789. [PubMed: 21746880]
45. Thiery JP, Sleeman JP. Complex networks orchestrate epithelial-mesenchymal transitions. Nature reviews. Molecular cell biology. 2006; 7:131–142. [PubMed: 16493418]
46. Matsubara T, Kida K, Yamaguchi A, Hata K, Ichida F, Meguro H, Aburatani H, Nishimura R, Yoneda T. BMP2 regulates Osterix through Msx2 and Runx2 during osteoblast differentiation. J Biol Chem. 2008; 283:29119–29125. [PubMed: 18703512]
47. Miyazono K, Kamiya Y, Morikawa M. Bone morphogenetic protein receptors and signal transduction. Journal of biochemistry. 2010; 147:35–51. [PubMed: 19762341]
48. Habibovic P, Bassett DC, Doillon CJ, Gerard C, McKee MD, Barralet JE. Collagen biomineralization in vivo by sustained release of inorganic phosphate ions. Adv Mater. 2010; 22:1858–1862. [PubMed: 20512962]
49. Murshed M, McKee MD. Molecular determinants of extracellular matrix mineralization in bone and blood vessels. Curr Opin Nephrol Hypertens. 2010; 19:359–365. [PubMed: 20489614]
50. Khan SR, Rodriguez DE, Gower LB, Monga M. Association of Randall plaque with collagen fibers and membrane vesicles. J Urol. 2012; 187:1094–1100. [PubMed: 22266007]
51. Lomashvili KA, Cobbs S, Hennigar RA, Hardcastle KI, O'Neill WC. Phosphate-induced vascular calcification: role of pyrophosphate and osteopontin. J Am Soc Nephrol. 2004; 15:1392–1401. [PubMed: 15153550]

52. Lomashvili KA, Garg P, Narisawa S, Millan JL, O'Neill WC. Upregulation of alkaline phosphatase and pyrophosphate hydrolysis: potential mechanism for uremic vascular calcification. Kidney Int. 2008; 73:1024–1030. [PubMed: 18288101]
53. Liu TM, Lee EH. Transcriptional regulatory cascades in Runx2-dependent bone development, Tissue engineering. Part B. Reviews. 2013; 19:254–263.
54. Liu W, Toyosawa S, Furuichi T, Kanatani N, Yoshida C, Liu Y, Himeno M, Narai S, Yamaguchi A, Komori T. Overexpression of Cbfa1 in osteoblasts inhibits osteoblast maturation and causes osteopenia with multiple fractures. The Journal of cell biology. 2001; 155:157–166. [PubMed: 11581292]
55. Khan SR, Glenton PA, Byer KJ. Modeling of hyperoxaluric calcium oxalate nephrolithiasis: experimental induction of hyperoxaluria by hydroxy-L-proline. Kidney Int. 2006; 70:914–923. [PubMed: 16850024]
56. Zuo J, Khan A, Glenton PA, Khan SR. Effect of NADPH oxidase inhibition on the expression of kidney injury molecule and calcium oxalate crystal deposition in hydroxy-L-proline-induced hyperoxaluria in the male Sprague-Dawley rats. Nephrol Dial Transplant. 2011; 26:1785–1796. [PubMed: 21378157]
57. Joshi S, Saylor BT, Wang W, Peck AB, Khan SR. Apocynin-treatment reverses hyperoxaluria induced changes in NADPH oxidase system expression in rat kidneys: a transcriptional study. PloS one. 2012; 7:e47738. [PubMed: 23091645]
58. Huang da W, Sherman BT, Lempicki RA. Bioinformatics enrichment tools: paths toward the comprehensive functional analysis of large gene lists. Nucleic acids research. 2009; 37:1–13. [PubMed: 19033363]
59. Huang da W, Sherman BT, Lempicki RA. Systematic and integrative analysis of large gene lists using DAVID bioinformatics resources. Nature protocols. 2009; 4:44–57. [PubMed: 19131956]
60. Khan SR. Reactive oxygen species as the molecular modulators of calcium oxalate kidney stone formation: evidence from clinical and experimental investigations. J Urol. 2013; 189:803–811. [PubMed: 23022011]
61. Evan AP, Lingeman JE, Coe FL, Parks JH, Bledsoe SB, Shao Y, Sommer AJ, Paterson RF, Kuo RL, Grynpas M. Randall's plaque of patients with nephrolithiasis begins in basement membranes of thin loops of Henle. J Clin Invest. 2003; 111:607–616. [PubMed: 12618515]
62. Stoller ML, Meng MV, Abrahams HM, Kane JP. The primary stone event: a new hypothesis involving a vascular etiology. J Urol. 2004; 171:1920–1924. [PubMed: 15076312]
63. Ando R, Nagaya T, Suzuki S, Takahashi H, Kawai M, Okada A, Yasui T, Kubota Y, Umemoto Y, Tozawa K, Kohri K. Kidney stone formation is positively associated with conventional risk factors for coronary heart disease in Japanese men. J Urol. 2013; 189:1340–1346. [PubMed: 23159273]
64. Bagga HS, Chi T, Miller J, Stoller ML. New insights into the pathogenesis of renal calculi. Urol Clin North Am. 2013; 40:1–12. [PubMed: 23177630]
65. Zhu D, Mackenzie NC, Shanahan CM, Shroff RC, Farquharson C, MacRae VE. BMP-9 regulates the osteoblastic differentiation and calcification of vascular smooth muscle cells through an ALK1 mediated pathway. Journal of cellular and molecular medicine. 2014
66. Wu XR. Interstitial calcinosis in renal papillae of genetically engineered mouse models: relation to Randall's plaques. Urolithiasis. 2015; 43(Suppl 1):65–76. [PubMed: 25096800]
67. de Water R, Leenen PJ, Noordermeer C, Nigg AL, Houtsmuller AB, Kok DJ, Schroder FH. Cytokine production induced by binding and processing of calcium oxalate crystals in cultured macrophages. Am J Kidney Dis. 2001; 38:331–338. [PubMed: 11479159]
68. de Water R, Noordermeer C, Houtsmuller AB, Nigg AL, Stijnen T, Schroder FH, Kok DJ. Role of macrophages in nephrolithiasis in rats: an analysis of the renal interstitium. Am J Kidney Dis. 2000; 36:615–625. [PubMed: 10977795]
69. Khan SR, Shevock PN, Hackett RL. Acute hyperoxaluria, renal injury and calcium oxalate urolithiasis. J Urol. 1992; 147:226–230. [PubMed: 1729537]
70. McKee MD, Nanci A, Khan SR. Ultrastructural immunodetection of osteopontin and osteocalcin as major matrix components of renal calculi. J Bone Miner Res. 1995; 10:1913–1929. [PubMed: 8619372]

71. Khan SR. Crystal-induced inflammation of the kidneys: results from human studies, animal models, and tissue-culture studies. Clin Exp Nephrol. 2004; 8:75–88. [PubMed: 15235923]
72. Khan SR. Calcium oxalate crystal interaction with renal tubular epithelium, mechanism of crystal adhesion and its impact on stone development. Urol Res. 1995; 23:71–79. [PubMed: 7676537]
73. Koul HK, Koul S, Fu S, Santosham V, Seikhon A, Menon M. Oxalate: from crystal formation to crystal retention. J Am Soc Nephrol. 1999; 10(Suppl 14):S417–S421. [PubMed: 10541276]
74. Verkoelen CF, Schepers MS. Changing concepts in the aetiology of renal stones. Curr Opin Urol. 2000; 10:539–544. [PubMed: 11148722]
75. Koul S, Khandrika L, Meacham RB, Koul HK. Genome wide analysis of differentially expressed genes in HK-2 cells, a line of human kidney epithelial cells in response to oxalate. PloS one. 2012; 7:e43886. [PubMed: 23028475]
76. Lieske JC, Deganello S, Toback FG. Cell-crystal interactions and kidney stone formation. Nephron. 1999; 81(Suppl 1):8–17. [PubMed: 9873209]
77. Thamilselvan S, Byer KJ, Hackett RL, Khan SR. Free radical scavengers, catalase and superoxide dismutase provide protection from oxalate-associated injury to LLC-PK1 and MDCK cells. J Urol. 2000; 164:224–229. [PubMed: 10840464]
78. Thamilselvan S, Hackett RL, Khan SR. Lipid peroxidation in ethylene glycol induced hyperoxaluria and calcium oxalate nephrolithiasis. J Urol. 1997; 157:1059–1063. [PubMed: 9072543]
79. Cao LC, Honeyman TW, Cooney R, Kennington L, Scheid CR, Jonassen JA. Mitochondrial dysfunction is a primary event in renal cell oxalate toxicity. Kidney Int. 2004; 66:1890–1900. [PubMed: 15496160]
80. Niimi K, Yasui T, Hirose M, Hamamoto S, Itoh Y, Okada A, Kubota Y, Kojima Y, Tozawa K, Sasaki S, Hayashi Y, Kohri K. Mitochondrial permeability transition pore opening induces the initial process of renal calcium crystallization. Free Radic Biol Med. 2012; 52:1207–1217. [PubMed: 22285391]
81. Khand FD, Gordge MP, Robertson WG, Noronha-Dutra AA, Hothersall JS. Mitochondrial superoxide production during oxalate-mediated oxidative stress in renal epithelial cells. Free Radic Biol Med. 2002; 32:1339–1350. [PubMed: 12057772]
82. Meimaridou E, Lobos E, Hothersall JS. Renal oxidative vulnerability due to changes in mitochondrial-glutathione and energy homeostasis in a rat model of calcium oxalate urolithiasis. Am J Physiol Renal Physiol. 2006; 291:F731–F740. [PubMed: 16670437]
83. Khan SR, Khan A, Byer KJ. Temporal changes in the expression of mRNA of NADPH oxidase subunits in renal epithelial cells exposed to oxalate or calcium oxalate crystals. Nephrol Dial Transplant. 2011; 26:1778–1785. [PubMed: 21079197]
84. Thamilselvan V, Menon M, Thamilselvan S. Oxalate-induced activation of PKC-alpha and -delta regulates NADPH oxidase-mediated oxidative injury in renal tubular epithelial cells. Am J Physiol Renal Physiol. 2009; 297:F1399–F1410. [PubMed: 19692488]
85. Hammes MS, Lieske JC, Pawar S, Spargo BH, Toback FG. Calcium oxalate monohydrate crystals stimulate gene expression in renal epithelial cells. Kidney Int. 1995; 48:501–509. [PubMed: 7564119]
86. Koul H, Kennington L, Honeyman T, Jonassen J, Menon M, Scheid C. Activation of c-myc gene mediates the mitogenic effects of oxalate in LLC-PK1 cells, a line of renal epithelial cells. Kidney Int. 1996; 50:1525–1530. [PubMed: 8914018]
87. Khan SR, Kok DJ. Modulators of urinary stone formation. Front Biosci. 2004; 9:1450–1482. [PubMed: 14977559]
88. Khan SR, Joshi S, Wang W, Peck AB. Regulation of macromolecular modulators of urinary stone formation by reactive oxygen species: transcriptional study in an animal model of hyperoxaluria. Am J Physiol Renal Physiol. 2014; 306:F1285–F1295. [PubMed: 24598804]
89. Miyazawa K, Aihara K, Ikeda R, Moriyama MT, Suzuki K. cDNA macroarray analysis of genes in renal epithelial cells exposed to calcium oxalate crystals. Urol Res. 2009; 37:27–33. [PubMed: 19066878]
90. Chen NX, Moe SM. Vascular calcification: pathophysiology and risk factors. Curr Hypertens Rep. 2012; 14:228–237. [PubMed: 22476974]

91. Smith N, Dong Y, Lian JB, Pratap J, Kingsley PD, van Wijnen AJ, Stein JL, Schwarz EM, O'Keefe RJ, Stein GS, Drissi MH. Overlapping expression of Runx1(Cbfa2) and Runx2(Cbfa1) transcription factors supports cooperative induction of skeletal development. Journal of cellular physiology. 2005; 203:133–143. [PubMed: 15389629]
92. Lee KS, Kim HJ, Li QL, Chi XZ, Ueta C, Komori T, Wozney JM, Kim EG, Choi JY, Ryoo HM, Bae SC. Runx2 is a common target of transforming growth factor beta1 and bone morphogenetic protein 2, and cooperation between Runx2 and Smad5 induces osteoblast-specific gene expression in the pluripotent mesenchymal precursor cell line C2C12. Molecular and cellular biology. 2000; 20:8783–8792. [PubMed: 11073979]
93. Yang X, Meng X, Su X, Mauchley DC, Ao L, Cleveland JC Jr, Fullerton DA. Bone morphogenic protein 2 induces Runx2 and osteopontin expression in human aortic valve interstitial cells: role of Smad1 and extracellular signal-regulated kinase 1/2. The Journal of thoracic and cardiovascular surgery. 2009; 138:1008–1015. [PubMed: 19664780]
94. Kawata T, Nagano N, Obi M, Miyata S, Koyama C, Kobayashi N, Wakita S, Wada M. Cinacalcet suppresses calcification of the aorta and heart in uremic rats. Kidney Int. 2008; 74:1270–1277. [PubMed: 18813289]
95. Zhang C. Transcriptional regulation of bone formation by the osteoblast-specific transcription factor Osx. Journal of orthopaedic surgery and research. 2010; 5:37. [PubMed: 20550694]
96. Mizuhashi K, Kanamoto T, Ito M, Moriishi T, Muranishi Y, Omori Y, Terada K, Komori T, Furukawa T. OBIF, an osteoblast induction factor, plays an essential role in bone formation in association with osteoblastogenesis. Development, growth & differentiation. 2012; 54:474–480.
97. Jang WG, Kim EJ, Kim DK, Ryoo HM, Lee KB, Kim SH, Choi HS, Koh JT. BMP2 protein regulates osteocalcin expression via Runx2-mediated Atf6 gene transcription. J Biol Chem. 2012; 287:905–915. [PubMed: 22102412]
98. Mandal CC, Ganapathy S, Gorin Y, Mahadev K, Block K, Abboud HE, Harris SE, Ghosh-Choudhury G, Ghosh-Choudhury N. Reactive oxygen species derived from Nox4 mediate BMP2 gene transcription and osteoblast differentiation. Biochem J. 2011; 433:393–402. [PubMed: 21029048]
99. Jia Z, Wang S, Tang J, He D, Cui L, Liu Z, Guo B, Huang L, Lu Y, Hu H. Does crystal deposition in genetic hypercalciuric rat kidney tissue share similarities with bone formation? Urology. 2014; 83:509, e507–e514. [PubMed: 24468523]
100. Liu Y. Epithelial to mesenchymal transition in renal fibrogenesis: pathologic significance, molecular mechanism, and therapeutic intervention. J Am Soc Nephrol. 2004; 15:1–12. [PubMed: 14694152]
101. Wang W, Li C, Pang L, Shi C, Guo F, Chen A, Cao X, Wan M. Mesenchymal stem cells recruited by active TGFbeta contribute to osteogenic vascular calcification. Stem cells and development. 2014; 23:1392–1404. [PubMed: 24512598]
102. Khan SR. Animal models of kidney stone formation: an analysis. World J Urol. 1997; 15:236–243. [PubMed: 9280052]
103. Khan SR. Nephrocalcinosis in animal models with and without stones. Urol Res. 2010; 38:429–438. [PubMed: 20658131]
104. Kumar V, Farell G, Yu S, Harrington S, Fitzpatrick L, Rzewuska E, Miller VM, Lieske JC. Cell biology of pathologic renal calcification: contribution of crystal transcytosis, cell-mediated calcification, and nanoparticles. J Investig Med. 2006; 54:412–424.

Highlights

First robust demonstration of the possible evolution of tubular epithelial cells to osteoblast-like cells.

Hyperoxaluria causes up regulation of genes for runt related transcription factors (RUNX) and zinc finger protein Osterix in kidneys of hyperoxaluric kidneys.

Hyperoxaluria causes up regulation of genes for bone morphogenetic proteins (BMP2 and 7), bone morphogenetic protein receptor(BMPR2), collagen, osteocalcin, osteonectin, osteopontin (OPN), matrix-gla-protein (MGP), osteoprotegrin (OPG), cadherins, fibronectin (FN) and vimentin (VIM).

Hyperoxaluria causes down regulation of genes for alkaline phosphatase (ALP) and cytokeratins 10 and 18.

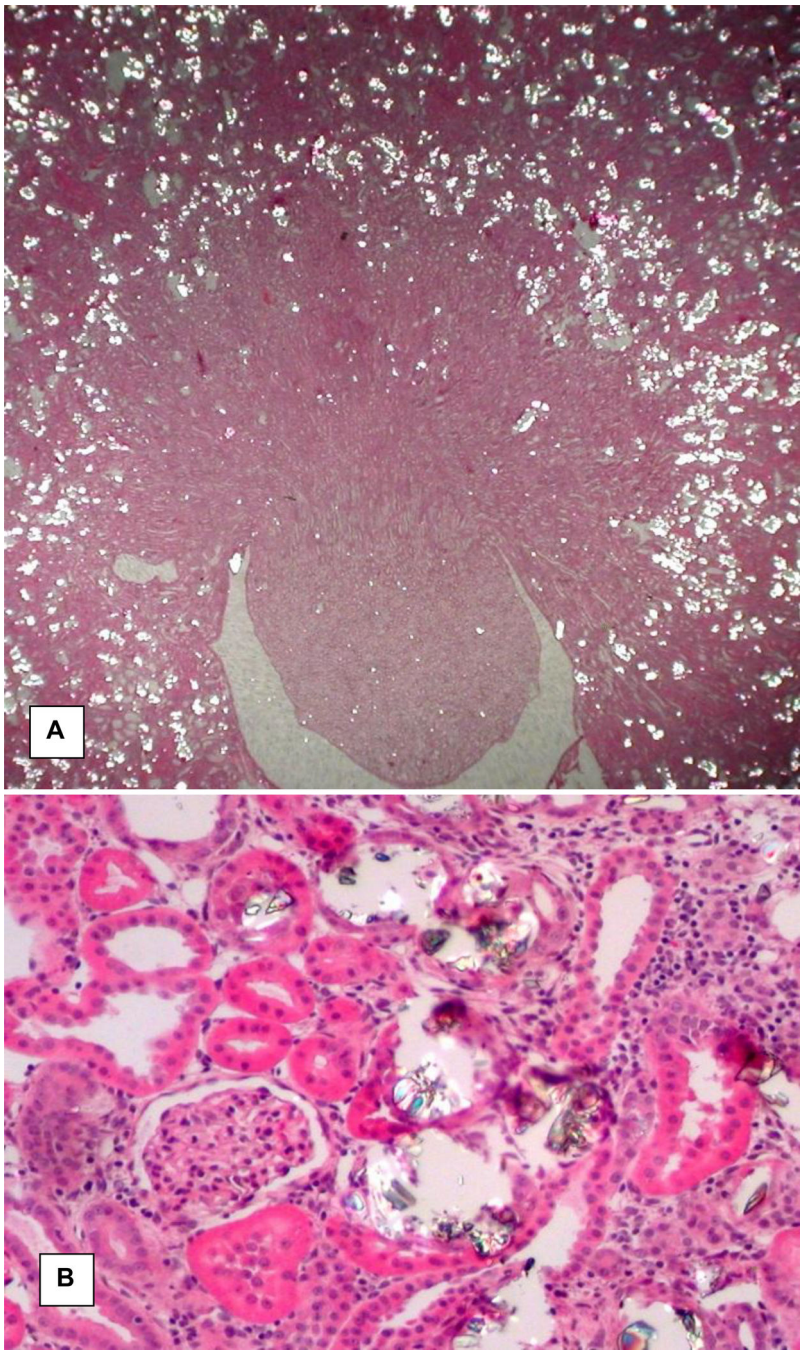

Figure 1.

H&A stained section of a kidney from hyperoxaluric rat on 28th day of feeding on hydroxyl-L-proline (HLP). **A**. Low mag image showing both cortical and medullary segments of the kidney. Calcium oxalate (CaOx) crystal deposits appear as bright spots and most of them are located in the cortical renal tubules. Original ×2.5. **B**. High magnification image showing a glomerulus and tubules with and without CaOx crystals. Glomerulus and tubules without the crystals appear normal. Tubules with crystals are dilated with many fold increase in their

luminal diameter and compressed lining epithelia. Renal interstitium shows signs of inflammation. Original ×45.

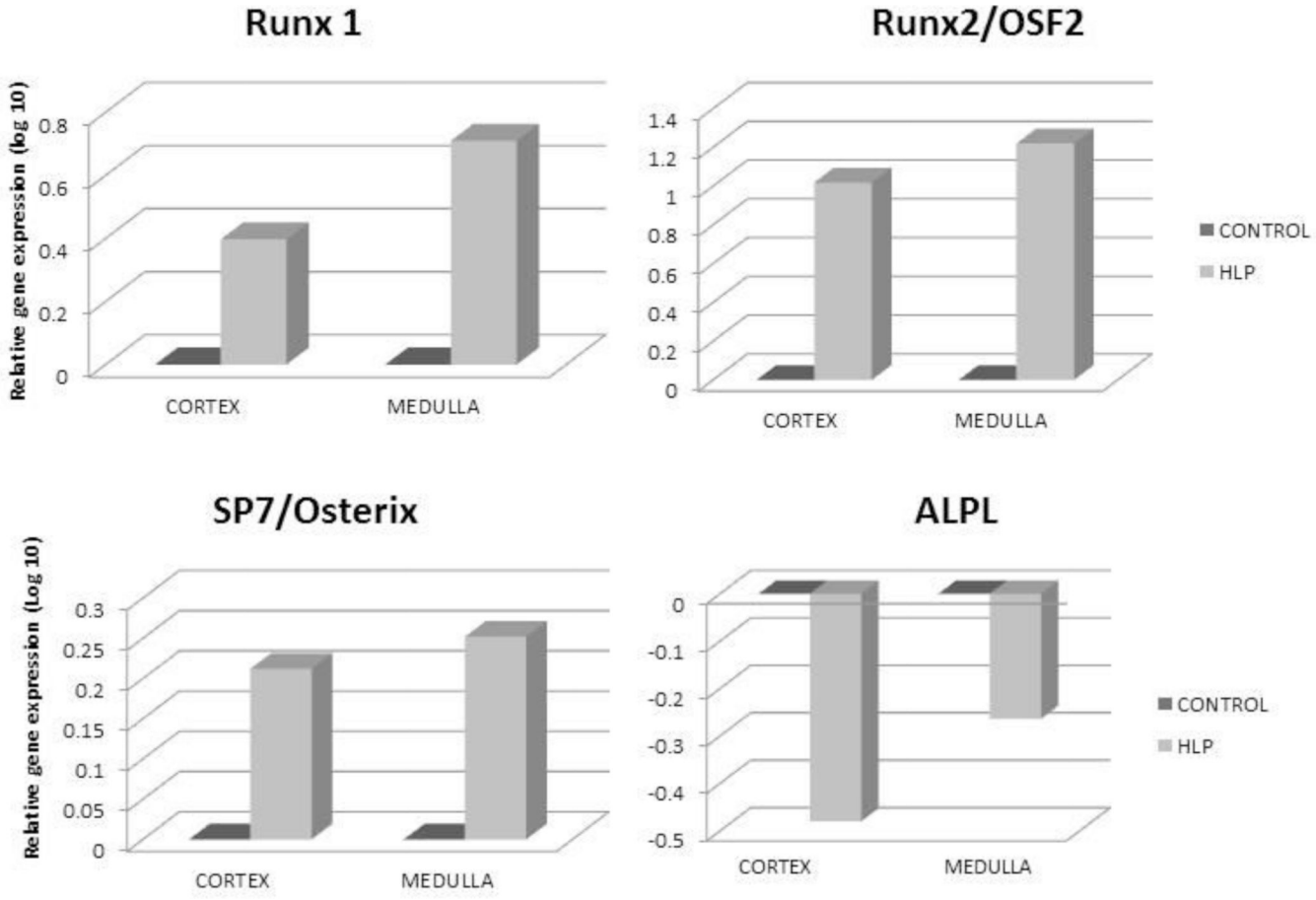

Figure 2.

Relative gene expression in the cortex and medulla of kidneys of control and HLP-fed rats. Gene expression of runt related transcription factor-1 and 2 (RUNX1 and RUNX2), and zinc finger protein Osterix/SP7was up regulated in the HLP-fed rats. Genes for alkaline phosphatase were downregulated in both cortex and medulla of the HLP-fed rats.

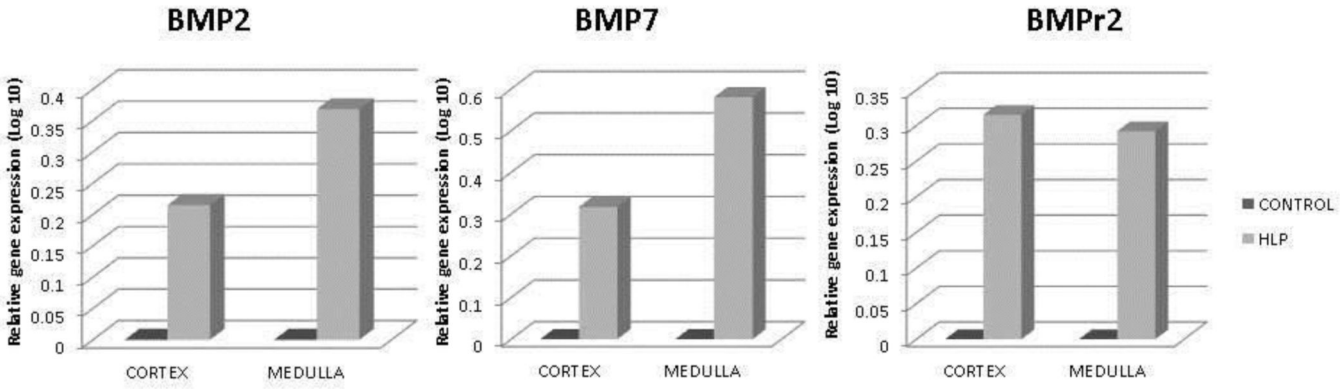

Figure 3.

Relative gene expression in the cortex and medulla of kidneys of control and HLP-fed rats. Gene expression of bone morphogenetic proteins 2 and 7 (BMP2 and BMP7), and bone morphogenetic protein receptor, Type 2 (BMPR2) were up regulated in the HLP- fed rats.

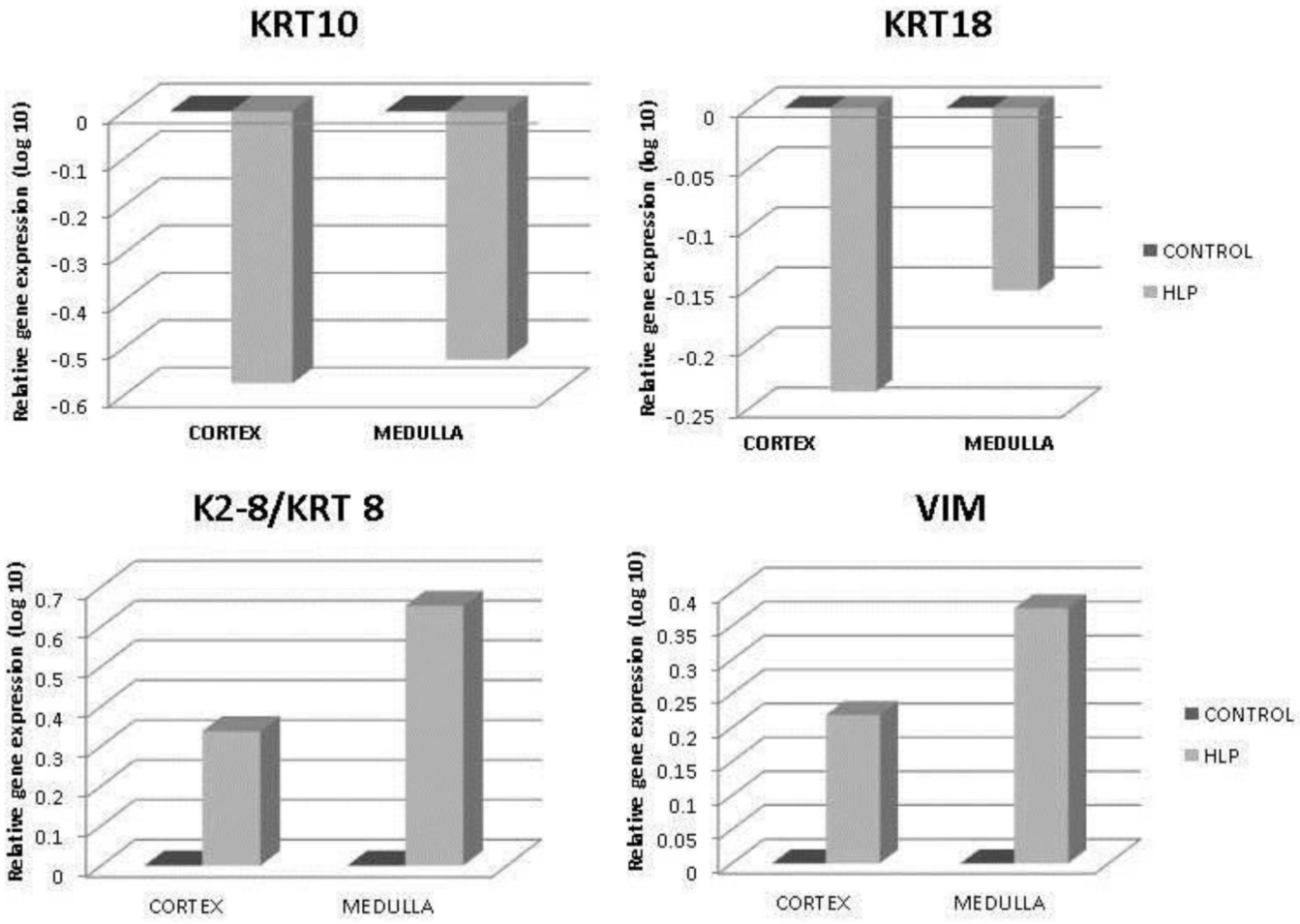

Figure 4.

Relative gene expression of cytokeratin 10 (KRT 10), cytokeratin 18 (KRT 18), cytokeratin 8 (KRT 8) and Vimentin (VIM) in the cortex and medulla of HLP treated rats. KRT10 and KRT18 gene expression was down regulated whereas KRT 8 and VIM were up regulated.

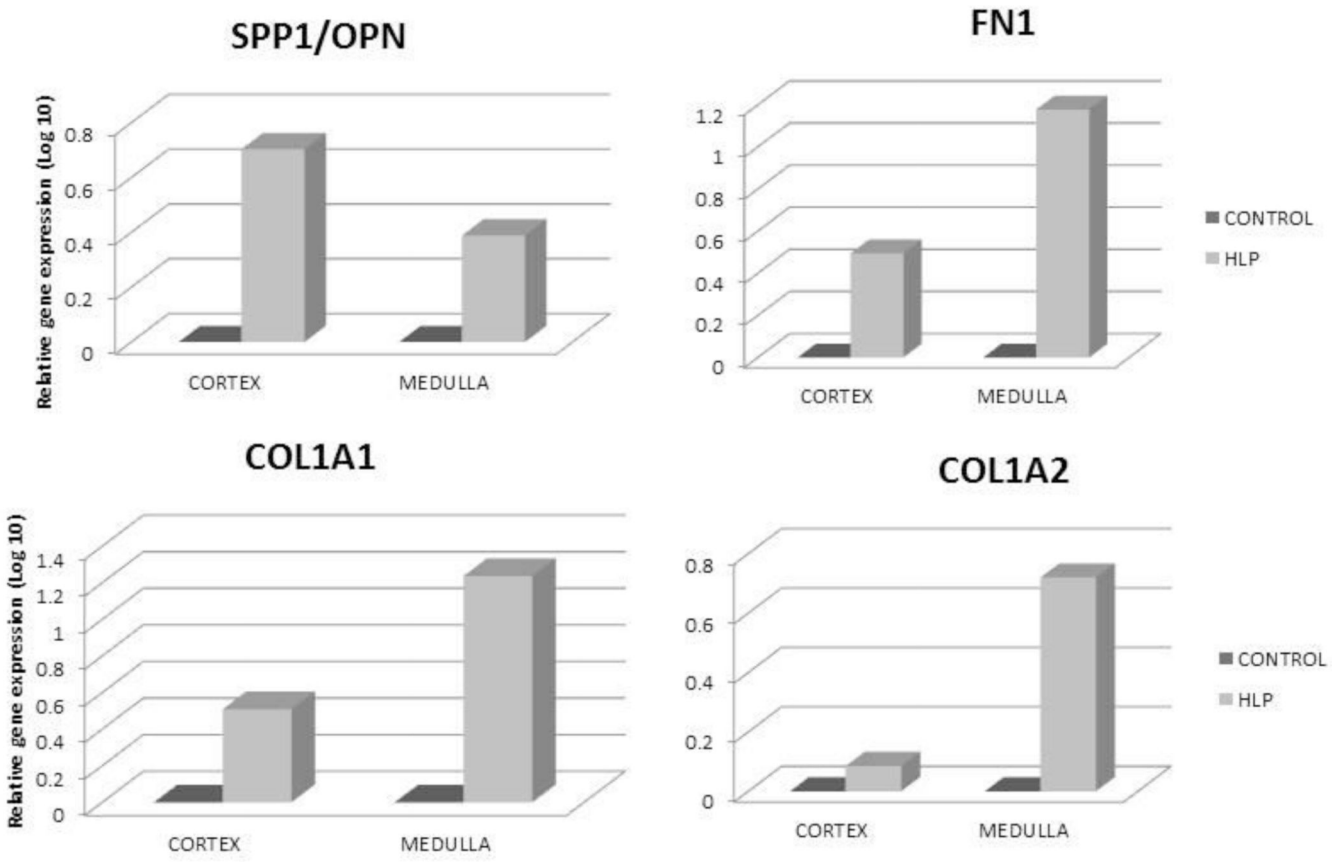

Figure 5.

Relative gene expression of OPN, Fibronectin (FN1), COL1A1 and COL1A2 in the cortex and medulla of HLP treated rats. Gene expressions were up regulated.

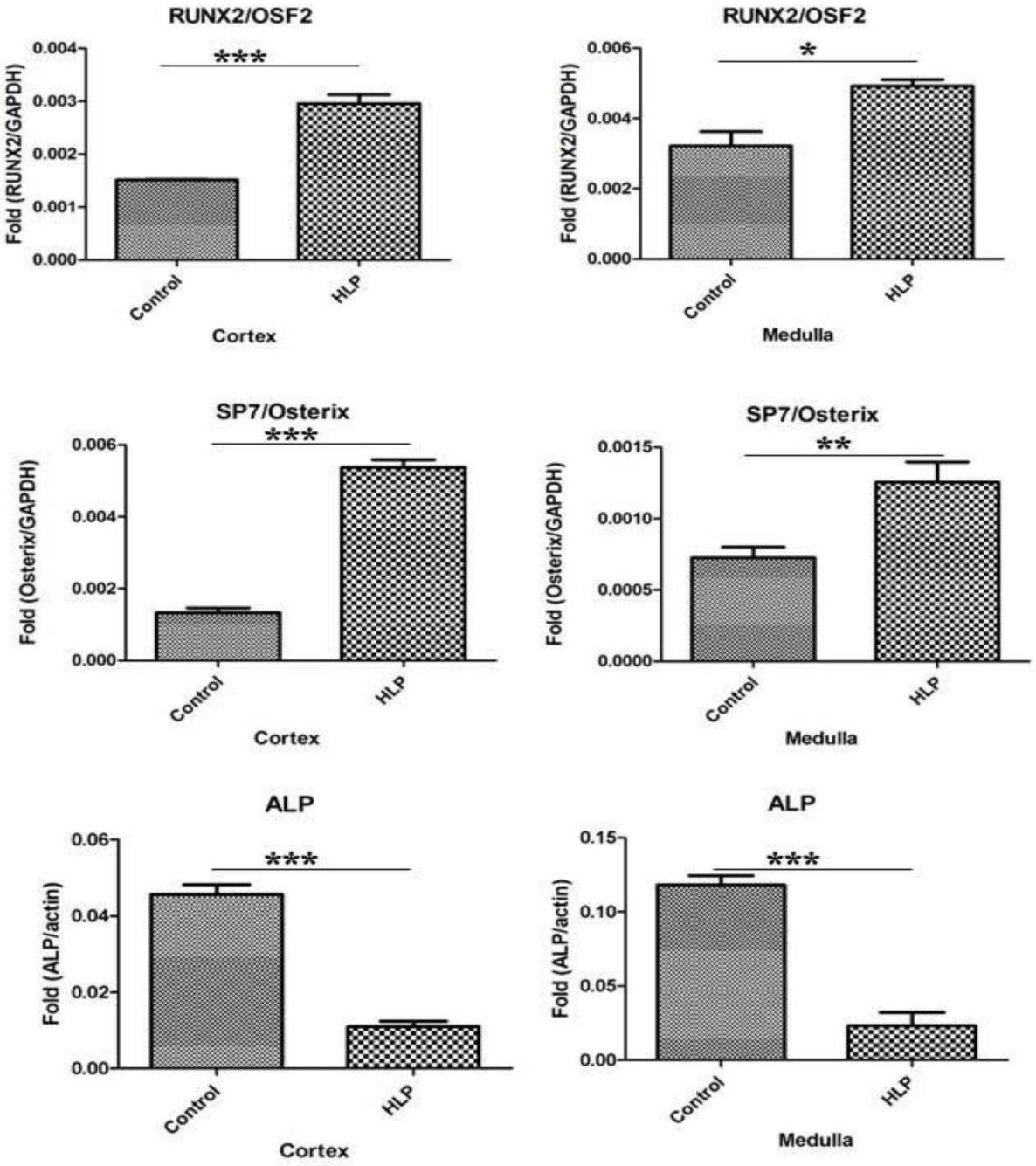

Figure 6.

Real Time PCR of runt related transcription factor-2 (RUNX2), zinc finger protein Osterix/SP7 and ALP in the cortex and medulla of the control and HLP fed rats. The statistical analyses were performed using GraphPad Prism version 5 for windows (GraphPad software, La Jolla, CA). P-values were calculated using unpaired T-test. $P < 0.05$ was considered statistically significant. *Control vs. HLP group ($P < 0.05$), **Control vs. HLP group ($P < 0.005$), ***Control vs. HLP group ($P < 0.0001$).

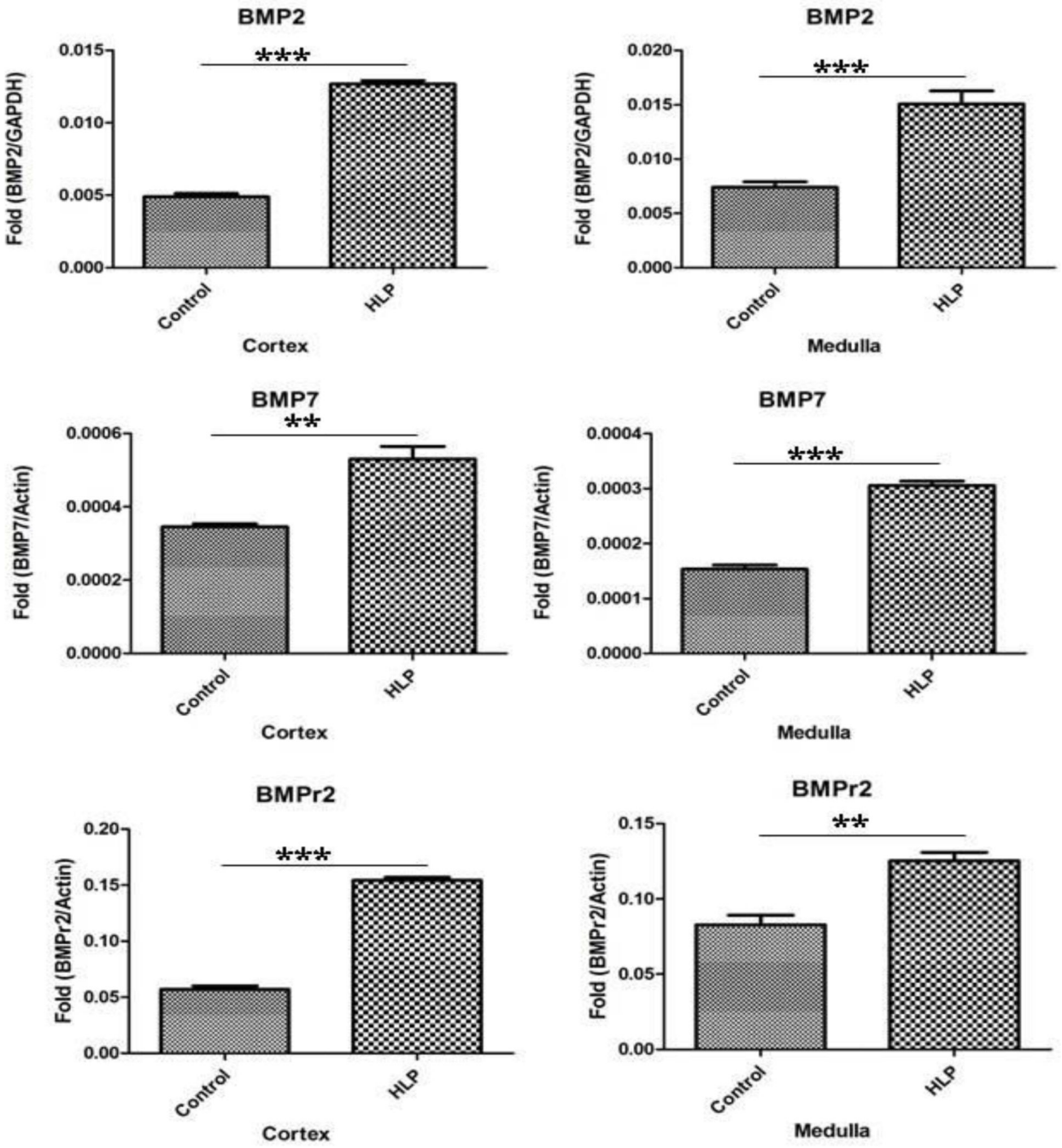

Figure 7.

Real Time PCR of bone morphogenetic proteins 2 (BMP2), bone morphogenetic proteins 7 (BMP7), and bone morphogenetic protein receptor, Type 2 (BMPR2) in the cortex and medulla of the control and HLP fed rats. The statistical analyses were performed using GraphPad Prism version 5 for windows (GraphPad software, La Jolla, CA). P-values were calculated using unpaired T-test. $P < 0.05$ was considered statistically significant. *Control vs. HLP group ($P < 0.05$), **Control vs. HLP group ($P < 0.005$), ***Control vs. HLP group ($P < 0.0001$).

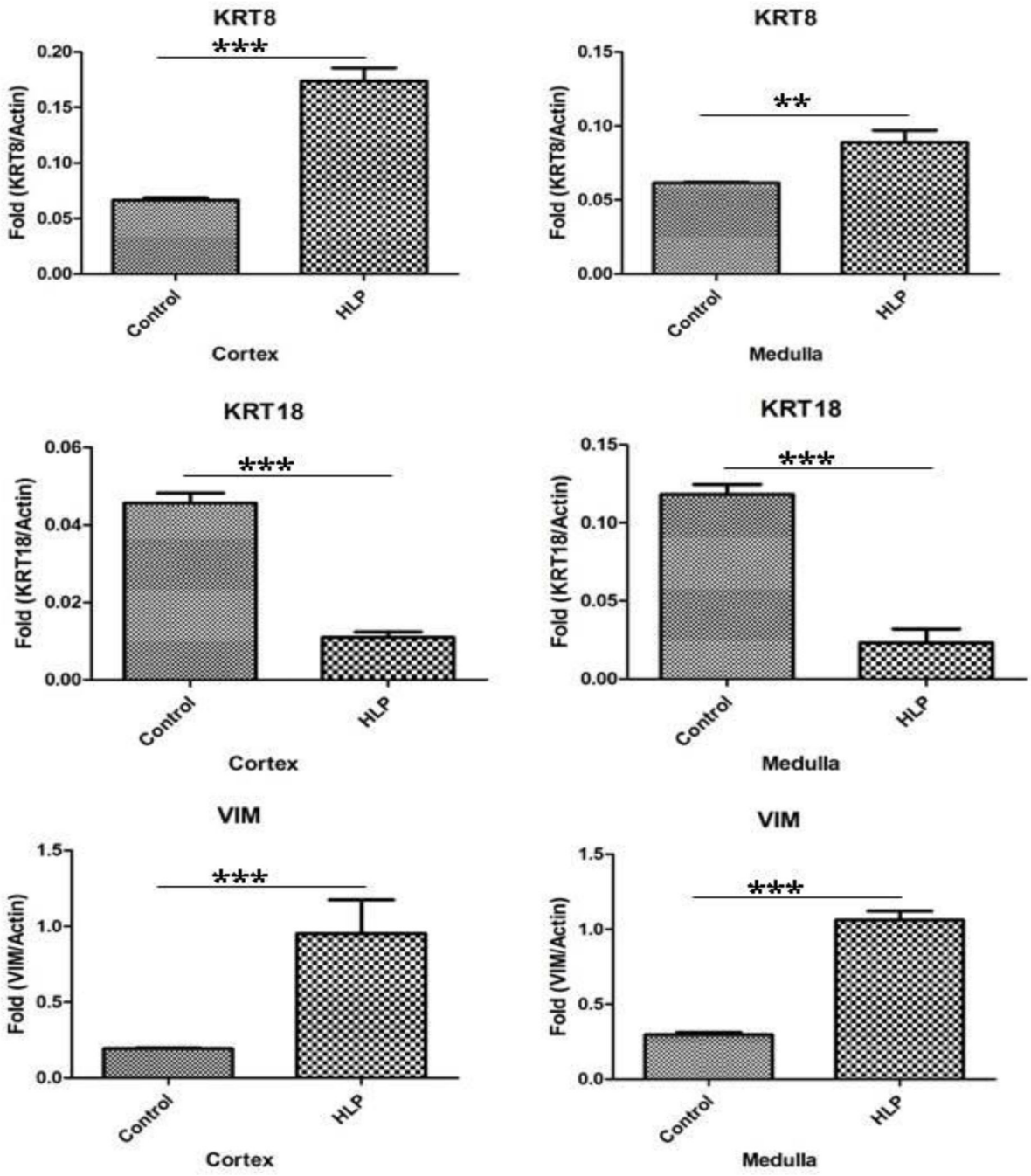

Figure 8.

Real Time PCR of cytokeratin 8 (KRT8), cytokeratin 18 (KRT18), and Vimentin (VIM) in the cortex and medulla of the control and HLP fed rats. The statistical analyses were performed using GraphPad Prism version 5 for windows (GraphPad software, La Jolla, CA). P-values were calculated using unpaired T-test. $P < 0.05$ was considered statistically significant. *Control vs. HLP group ($P < 0.05$), **Control vs. HLP group ($P < 0.005$), ***Control vs. HLP group ($P < 0.0001$).

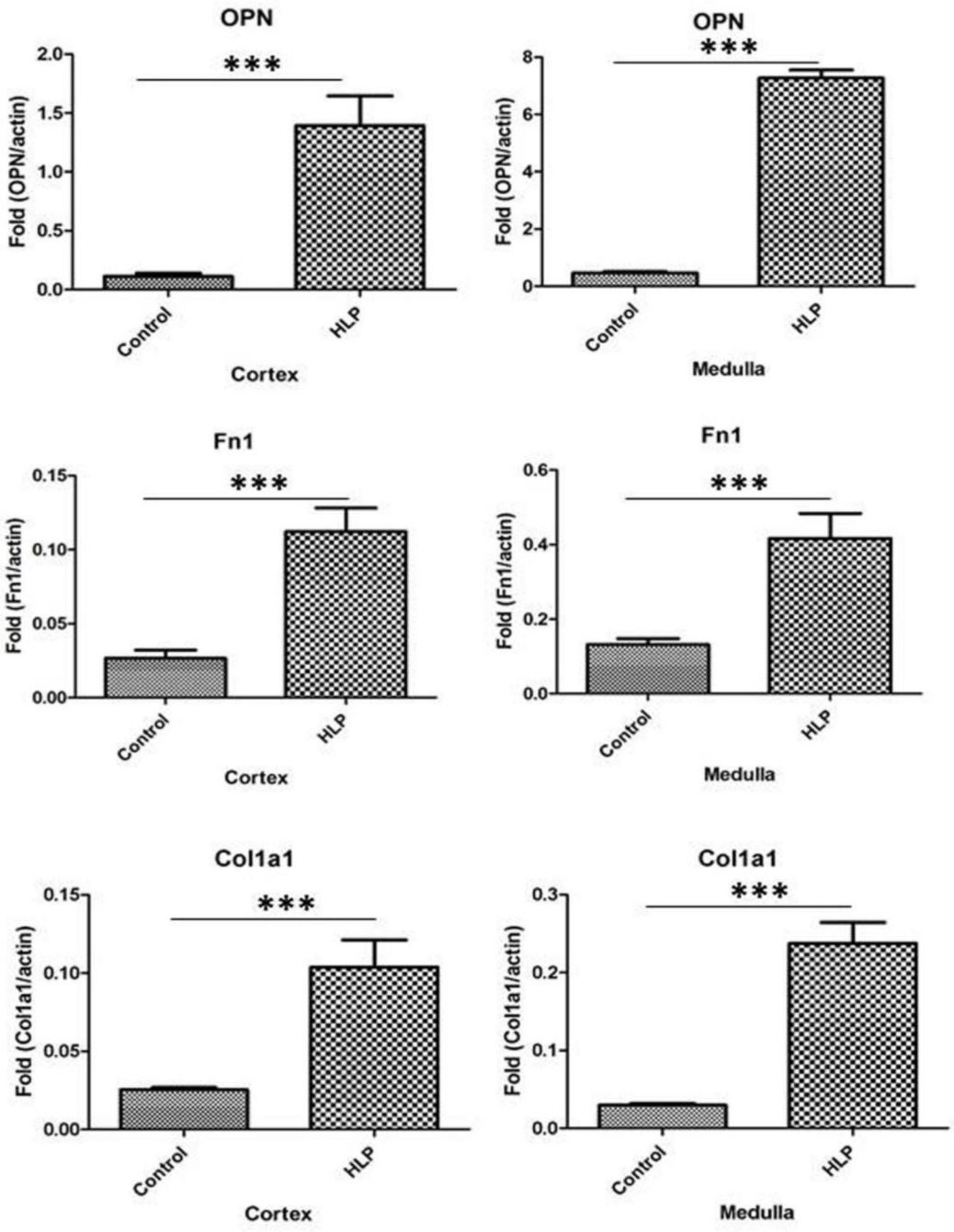

Figure 9.
Real time PCR of OPN, Fn1, Col 1a1 and Col 1a2 showing increase in their expressions.

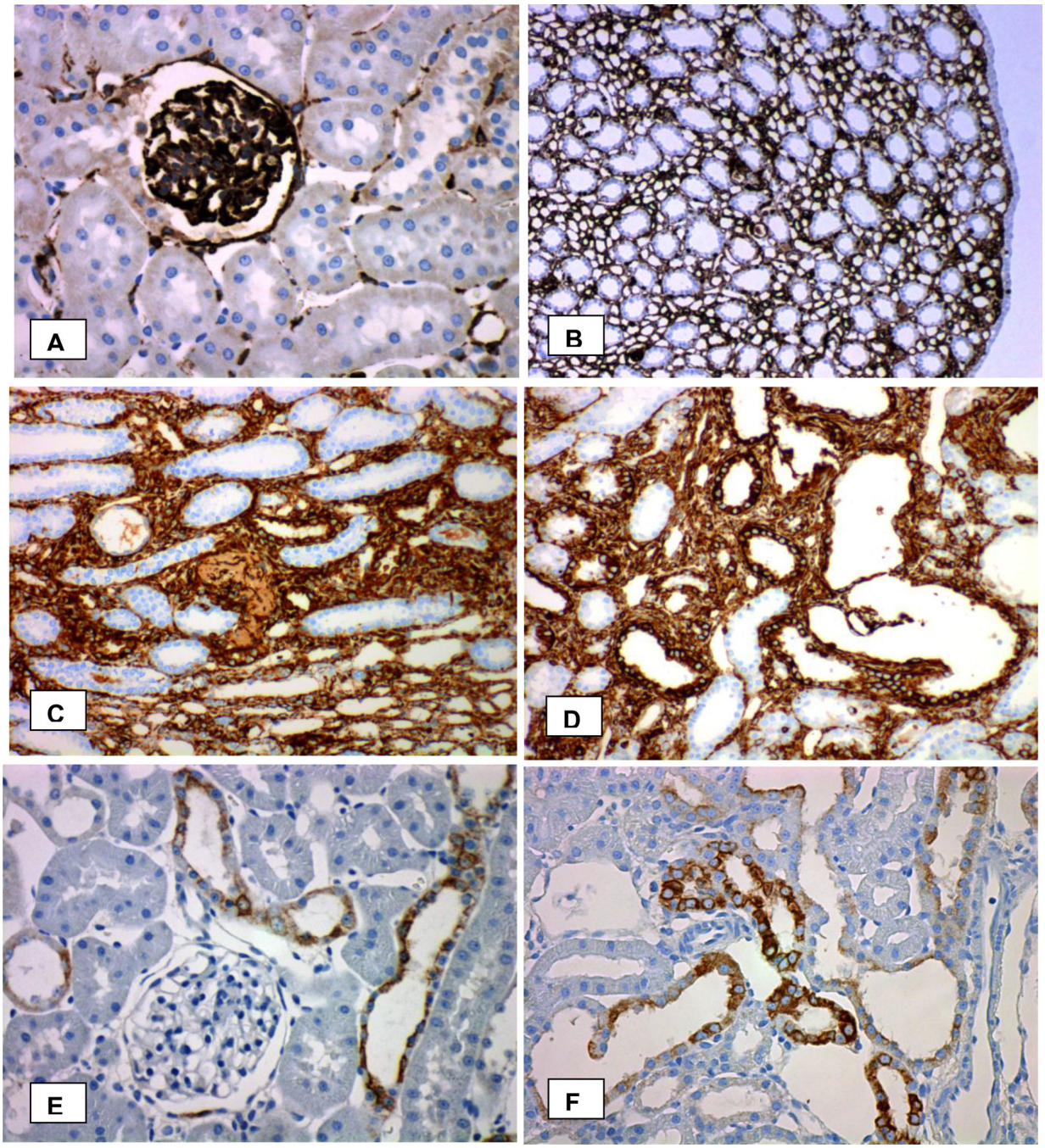

Figure 10.

Immunohistochemical analyses of the kidneys for vimentin and cytokeratin. **A**. Normal kidney cortex showing vimentin staining in the glomerulus and peritubular capillaries. **B**. Normal kidney papilla showing vimentin staining in the peritubular capillaries. **C, D**. Strong staining is seen for vimentin in the epithelial cells of the tubules with CaOx crystal deposits as well as the surrounding renal interstitium. **E**. Stainining with pancytokeratin antibody in normal kidney cortex. **F**. Stainining with pancytokeratin antibody in cortex of a kidney from HLP-fed rats. Original Mag ×45.

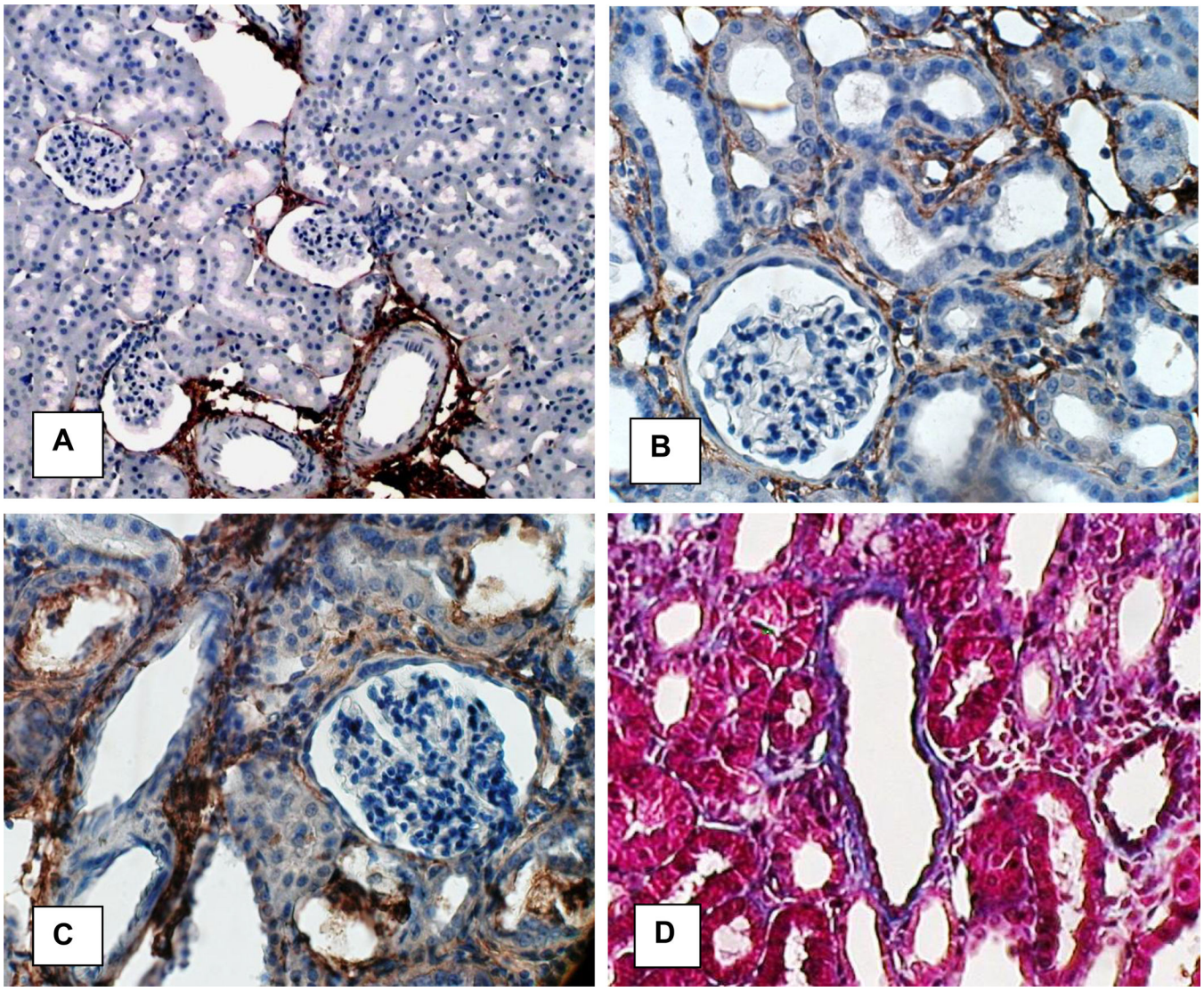

Figure 11.

Immunohistochemical analyses of the kidneys of control and HLP-fed rats for collagen. **A** In normal Collagen 1 expression is mostly limited to areas around large and small blood vessels. Original Mag ×10. B. C. In hyperoxaluric kidneys Collagen 1 expression is interstitial and more intense around tubules with CaOx crysral deposits. Crystals have been lost during the processing. D. Collagen stained blue with Mason's trichrome. There is strong staining around the tubules with CaOx crystal deposits. Epithelial cells of the tubules without crystals stained red. Original Mag ×45.

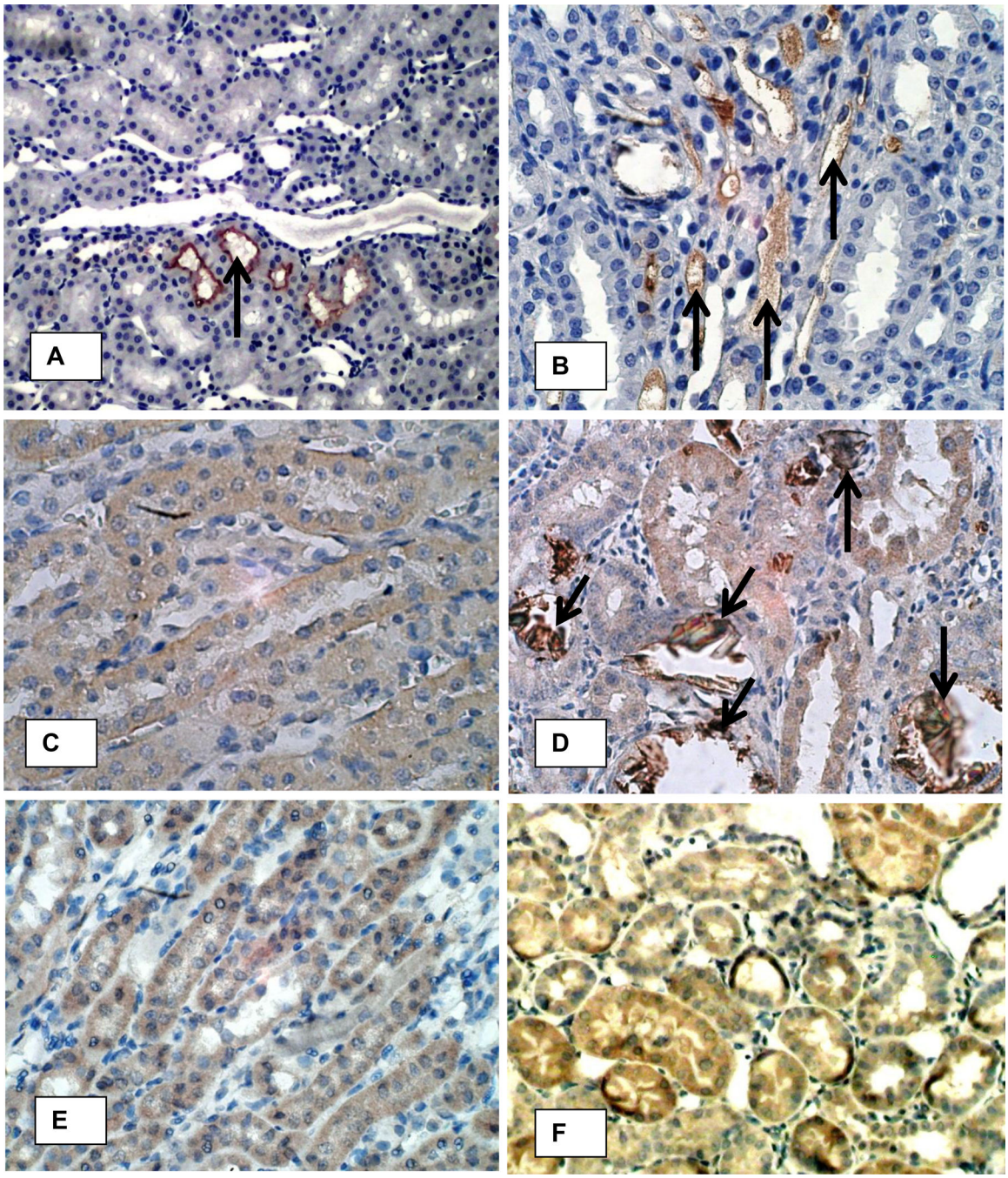

Figure 12.

Immunohistochemical analyses of the kidneys of control (A, C, E) and HLP-fed rats (B, D, F) for MGP, OPN and fibronectin. A. Only nonspecific staining for MGP was seen (arrow) in normal rat kidneys. **B**. MGP staining was markedly increased in the peritubular vessels (arrows) of the kidneys of hyperoxaluric rats (atrrows). C. OPN staining was not seen in the normal kidneys except on the papillary urothelial surface (not shown). **D**. Staining of epithelial cells for osteopontin was mostly associated with crystal deposits (arrows). E. Diffuse light staining for fibronectin is seen in renal epithelial cells as well interstitium of

the normal kidneys. **F**. Intense fibronectin staining is seen in both the tubular epithelial cells as well as interstitium of the kidneys with hyperoxaluria. Original Mag ×45.

Table 1

The list of forward and reverse primers used for quantitative Real Time PCR designed using Primer-BLAST (National Center for Biotechnology Information, NCBI, and National Institute of Health, NIH)

GENE	PRIMER	SEQUENCE
Fibronectin (*Fn1*)	Fn1_F	5'- GTGGCTGCCTTCAACTTCTC-3'
	Fn1_R	5'- GTGGGTTGCAAACCTTCAAT-3'
Runt-related transcription factor-2 (*Runx2*)	Runx2_F	5'- TCCCATCTGCTAGAAGTGTT-3'
	Runx2_R	5'- TTAGCCAGCTCACTTTCTTC-3'
Osterix/SP7	Sp7_F	5'- AAGCCATACACTGACCTTTC-3'
	Sp7_R	5'- GTGGGTAGTCATTGGCATAG-3'
Bone Morphogenetic Protein-2 (*Bmp2*)	Bmp2_F	5'- ACCAGACTATTGGACACCAG-3'
	Bmp2_R	5'- AATCCTCACATGTCTCTTGG-3'
Bone Morphogenetic Protein-7 (*Bmp7*)	Bmp7_F	5'- ATGGCCAACGTGGCAGAGAA-3'
	Bmp7_R	5'- CAGCCCAGGTCTCGGAAGCT-3'
Bone Morphogenetic Protein Receptor, type II (*Bmpr2*)	Bmpr2_F	5'- ATAGGCGTGTGCCAAAAATC-3'
	Bmpr2_R	5'- GCTAGGGATTCGAGCTTGTG-3'
Cytokeratin 8 or Keratin 8 (*Krt8*)	Krt8_F	5'- AGCCAGAGTACCAGCCCTAA-3'
	Krt8_R	5'- ACAATTGAGTTGGGCATTGGC-3'
Cytokeratin 18 or Keratin 18 (*Krt18*)	Krt18_F	5'- ATATCCGTGTCCCGCTCTGT-3'
	Krt18_R	5'- TCGTTCAGGTCTTGCATGGT-3'
Vimentin (*Vim*)	Vim_F	5'- TTCTCAGCACCACGATGACC-3'
	Vim_R	5'- TGCTGAGCTCGTTTCTATCCC-3'